

## CORRELATION BETWEEN THE STRUCTURE IN THE LIQUID STATE AND THE STRUCTURE IN THE SOLID STATE IN THE Al–Al<sub>2</sub>Cu EUTECTIC ALLOY

S. Mudry<sup>1</sup>, I. Shtablavyi<sup>1</sup>, J. Rybicki<sup>2,3</sup>

<sup>1</sup>*Department for Metal Physics, Ivan Franko National University of Lviv,  
8, Kyryla i Mefodija St., Lviv, UA-79005, Ukraine*

<sup>2</sup>*Faculty of Technical Physics and Applied Mathematics,  
Gdansk University of Technology, Narutowicza St. 11/12, Gdansk, PL-80-233, Poland*

<sup>3</sup>*Institute of Mechatronics, Nanotechnology and Vacuum Technique,  
Koszalin University of Technology, Raclawicka St. 15-17, Koszalin, PL-75-620, Poland*

(Received October 25, 2010; received in final form March 15, 2011)

The structure of the Al<sub>0.83</sub>Cu<sub>0.17</sub> eutectic alloy in the liquid state was studied by means of the X-ray diffraction and molecular dynamics. The total and partial structure factors were analyzed and subsequently used to calculate the pair correlation functions and partial correlation functions, the analysis of which allowed us to conclude that Al<sub>2</sub>Cu-like atomic groups are formed and distributed in the Al matrix.

**Key words:** liquid alloys, structure factor, short-range order.

PACS number(s): 61.25.–F, 61.25.Mv, 61.43.Gt, 61.66.Dk, 62.23.Pq.

### I. INTRODUCTION

Al–Cu-based alloys are high-strength light mass structural materials that are used extensively in industry. The addition of copper as the main alloying element (usually at a concentration of 3–6 wt%, occasionally much higher) facilitates material strengthening by means of precipitation hardening, resulting in very strong alloys. Copper also improves the fatigue properties, high-temperature properties and the machinability of the alloy. Alloys containing 4–6 wt% Cu respond more strongly to thermal treatment [1, 2].

Lower levels of copper content are employed in the automotive industry. Such alloys are characterized by sufficient formability, spot weldability and good corrosion resistance (as opposed to alloys containing higher levels of copper).

The addition of copper, however, has an adverse impact on the corrosion resistance. Copper tends to precipitate at grain boundaries, making the metal highly susceptible to pitting, intergranular corrosion and stress corrosion.

Precipitation reactions in Al–Cu are rather complex. The equilibrium phase CuAl<sub>2</sub> is difficult to nucleate, and therefore its formation is preceded by a series of metastable precipitates. Guinier and Preston were the first to discover certain age-hardening phenomena [3, 4]. Thus, the first two precipitates to be formed in the sequence are known as Guinier–Preston zones (GP1 and GP2). GP1 consists of copper-rich plates 10 nm in diameter on {100}Al planes. These zones develop into GP2 zones, which also are coherent plates, 10 nm thick and 150 nm in diameter, leading to maximum hardening. Further on,  $\Theta'$  precipitates replace GP zones as semi-coherent particles, a process known as over-aging, since the hardness begins to decrease.

Thus, as we can see, the liquid-solid transition of Al–

Cu alloys is very complicated and therefore it is important to investigate such alloys, both in the liquid and the solid state.

### II. EXPERIMENTAL AND MODELLING

The samples under investigation were prepared in an arc melting furnace, filled with pure argon, from high-purity aluminium and copper (both 99.999%). The diffraction studies were carried out using a high-temperature diffractometer with a special attachment, which allows to investigate the solid and liquid samples at different temperatures, up to 1800 K. Cu–K $\alpha$  radiation, monochromatized by means of LiF single crystal as a monochromator and Bragg–Brentano focusing geometry were used. The scattered intensities were recorded as a function of the scattering angle with an angular step of 0.05° within the region of the principal peak and 0.5° for the remaining values of the wave vector. The measurement of the scattered intensity was performed with the accuracy of at least 2%. In order to obtain more accurate scattered intensities, the scan time was set at 100 s. The diffracted intensity was recorded using the NaI(Tl) scintillator detector together with the amplification system. The sample was placed in a rounded cup 20 mm in diameter. Intensity curves were corrected for polarization, absorption and incoherent scattering [5] and were subsequently normalized to electron units by the Krogh–Moe method [6]. The obtained intensity curves were used to calculate structure factors (SF), from which pair correlation functions (PCF) were calculated. The main structure parameters obtained from SF and PCF were subsequently analyzed.

Molecular dynamics (MD) simulations were performed using the nanoMD code, developed at the Gdańsk University of Technology [7–9]. The simulations were performed at a constant volume using the Nosé–Hoover

thermostat. The equations of motion were integrated with a fourth-order Gear predictor-corrector algorithm with a timestep of 2.5 fs. The Sutton–Chen (SC) potential [10,11], which has a simple power-law form and a relatively long-range character, was used. The system contained 10000 atoms and was initialized at a temperature of 2000 K and then cooled down to 835 K, passing the intermediate temperatures of 1800, 1600, 1400, 1200 and 1000 K. At each of these temperatures the melt was equilibrated for 50000 timesteps. Between the subsequent temperatures the system was cooled linearly at a rate of  $4 \times 10^{11}$  K/s.

### III. RESULTS AND DISCUSSION

The total structure factors for the  $\text{Al}_{0.83}\text{Cu}_{0.17}$  eutectic melt at the temperature of  $T_L + 5$  K ( $T_L = 825$  K) are shown in Fig. 1, contrasted with SFs for liquid Al and Cu. The main parameter — the principal peak position  $k_1$  for the eutectic melt was located between the respective peak positions for Al and Cu. The same observation was made in the case of the second maxima. It can be seen that the height of the principal peak in  $S(k)$  for the liquid eutectic is significantly lower than for the liquid components. This allows us to conclude that the degree of structural ordering in the liquid melt is lower than in the case of liquid copper and aluminum.

Similar features were also observed in the pair correlation functions. The interatomic distances  $r_1$  and  $r_2$  were different from the respective values for Al and Cu. The  $r_1$  was closer to the corresponding value for liquid Al, whereas  $r_2$  was closer to the one for Cu. The number of neighbors  $Z$  was lower than for Cu or Al. This allows us to conclude that the structure of molten eutectic alloy is different from that of a simple eutectic melt.

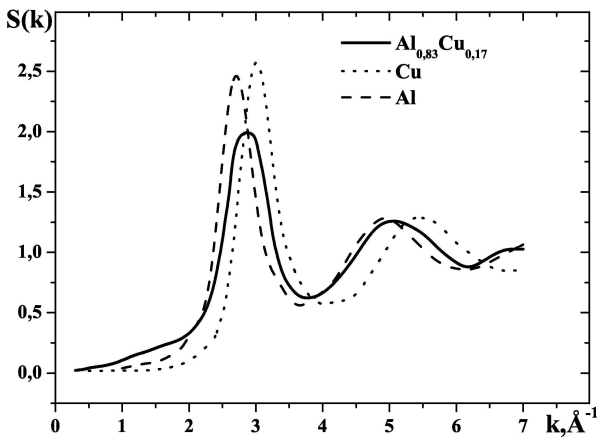


Fig. 1. Structure factors for the liquid  $\text{Al}_{0.83}\text{Cu}_{0.17}$  eutectic alloy, as compared with structure factors for liquid Al and Cu.

The structure of the molten  $\text{Al}_{0.83}\text{Cu}_{0.17}$  eutectic alloy is different from that of molten Al, even though Al prevails in the total composition. The small fraction of Cu atoms influences the atomic distribution of Al to a degree higher than would be expected for a simple solution

of copper in aluminum. Moreover, we suppose that the real structure of the molten eutectic may be somewhat different from the mixture of the  $\text{Cu}_n$  and  $\text{Al}_m$  structural units. In order to confirm this assumption, we calculated the structure factor, assuming additive scattering from both the Al and Cu regions (Fig. 2). The corresponding formula can be easily obtained, using the SFs of liquid aluminum and copper.

$$S(k) = C_{\text{Al}}K_{\text{Al}}^2S_{\text{Al}}(k) + C_{\text{Cu}}K_{\text{Cu}}^2S_{\text{Cu}}(k), \quad (1)$$

where  $C_{\text{Al}}$ ,  $C_{\text{Cu}}$  are the fractions of the aluminum and copper structural units;  $K_{\text{Al}}$ ,  $K_{\text{Cu}}$  are the respective scattering abilities.

As can be seen from Fig. 2, the calculated structure factor, which was obtained according to a weighted superposition of structure factors for Al and Cu, differs from the experimentally obtained one. First, the principal peak height of the calculated SF is significantly higher than that of  $S_{\text{exp}}(k)$ . A characteristic feature of the experimentally obtained SF is the presence of a shoulder in the low- $k$  region,  $k \approx 1.5 \text{ \AA}^{-1}$ . This shoulder is commonly interpreted as a manifestation of medium-range order [12].

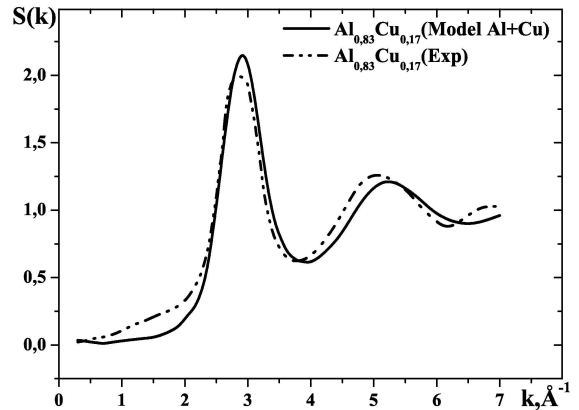


Fig. 2. Experimental and calculated structure factors of the liquid  $\text{Al}_{0.83}\text{Cu}_{0.17}$  eutectic alloy.

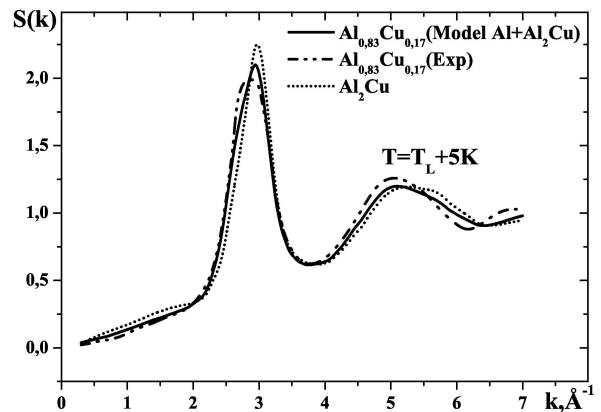


Fig. 3. Structure factors for the liquid  $\text{Al}_2\text{Cu}$  compound, as compared with the experimental SF of the liquid  $\text{Al}_{0.83}\text{Cu}_{0.17}$  eutectic alloy and the model structure factor obtained from a weighted superposition of structure factors for Al and  $\text{Al}_2\text{Cu}$ .

The presence of a prepeak in liquid Al-based alloys has been reported before by Maret *et al.* [14] for  $\text{Al}_{0.80}\text{Ni}_{0.20}$ , based on neutron diffraction. Using isotopic substitution, they attributed the prepeak to Ni–Ni pairs and interpreted it as resulting from a superstructure due to the preference for heteroatomic interactions. Their results were confirmed by Das *et al.* [15], who also performed neutron scattering experiments and, in addition, molecular dynamics simulation studies. In the case of the Al–Cu molten alloy, the intensity of this shoulder was maximum for the concentration corresponding to the  $\text{Al}_2\text{Cu}$  stoichiometric compound [13].

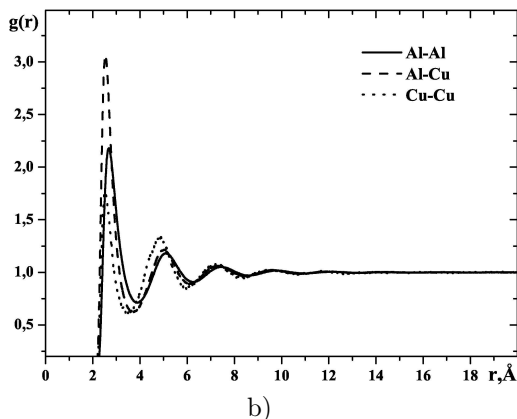
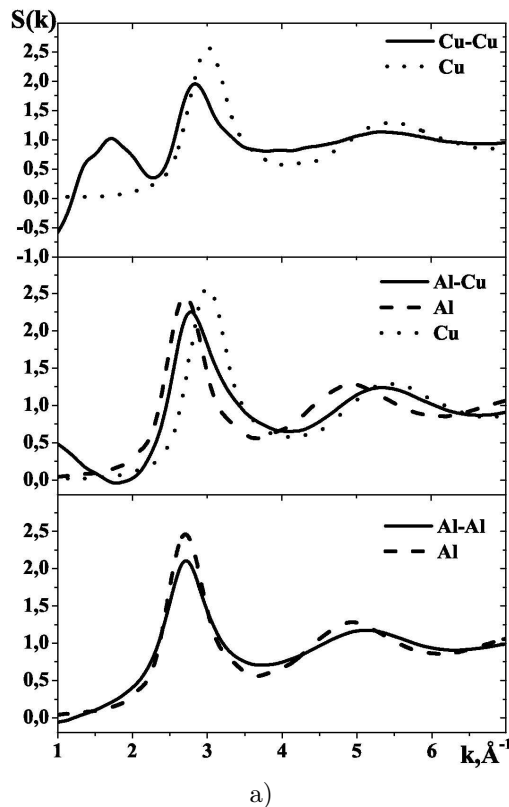


Fig. 4. The Faber-Ziman partial structure factors (a) and the partial pair correlation function (b) of the liquid  $\text{Al}_{0.83}\text{Cu}_{0.17}$  eutectic alloy (MD simulation).

Fig. 3 shows the structure factor for the  $\text{Al}_2\text{Cu}$  liquid alloy. The structure factor of this composition exhibits a distinct prepeak. Our results also indicate a similar

shoulder for the  $\text{Al}_{0.83}\text{Cu}_{0.17}$  eutectic, confirming the existence of chemically ordered nanogroups in this melt.

In order to resolve the abovementioned discrepancies between the experimental and model SFs, in this work we used another model, which assumes the existence of  $\text{Al}_2\text{Cu}$  clusters and Al-based structural units (Fig. 3). With this model, the discrepancy between the calculated and experimental values was less pronounced, lending credence to the presence of  $\text{Al}_2\text{Cu}$  nanogroups arranged in an Al matrix.

In order to confirm this hypothesis, the structure of the  $\text{Al}_{0.83}\text{Cu}_{0.17}$  eutectic melt was studied by means of molecular dynamics (MD). For the purposes of our calculations, a cubic cell containing 10000 atoms was chosen as the initial structural unit. The volume of this cell was determined from the experimental density. The calculated SF and the experimental one are in good agreement. The Faber-Ziman partial structure factors (PSFs) [16] and the partial pair correlation functions (PPCFs) were calculated (Fig. 4) from the model atomic configuration.

The PSFs related to the Al–Cu and Cu–Cu distributions exhibit certain features (intensity reduction and increase of the intensity, respectively) for wave vectors in the interval  $1\text{--}2 \text{ \AA}^{-1}$ . Such features were investigated in [14] and it was established that they are caused by the formation of substructure arising due to the preferred interaction of unlike atoms. The partial structure factor related to the Al–Al distribution resembles the structure factor of pure liquid aluminum, which is expected, as these atoms form a matrix containing the  $\text{Al}_2\text{Cu}$  nanogroups. On the other hand, the PSF describing the partial Cu–Cu atomic distribution differs significantly from the SF for liquid copper, indicating the disappearance of the Cu-like structure upon alloying.

The Al–Cu PSF shows the intermediate character compared to the structure factors of Al and Cu indicating a heterocoordinated atomic distribution.

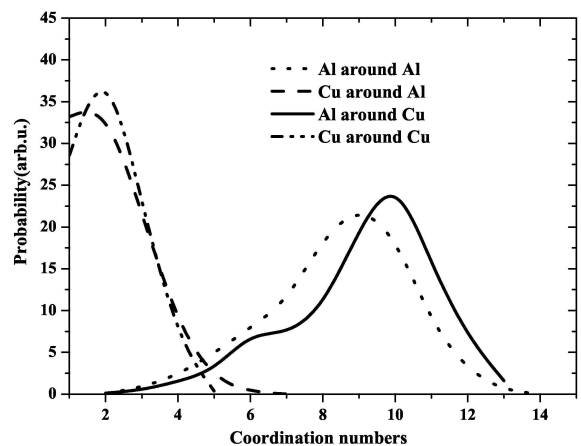


Fig. 5. The distribution of coordination numbers in the liquid  $\text{Al-Al}_2\text{Cu}$  alloy (MD simulation).

Figure 5 shows the distribution of the calculated partial coordination numbers in the liquid  $\text{Al}_{0.83}\text{Cu}_{0.17}$  eutectic alloy. The average coordination number of the liquid  $\text{Al}_{0.83}\text{Cu}_{0.17}$  is 10.4. The average Al–Al coordination number is 9, the coordination number for Al atoms

around central Cu atoms is 10. There is a small amount of Cu atoms (only two) around central Al atoms and Cu atoms around Cu ones (also only two). Furthermore, a shoulder in the region of 6–8 can be observed in the distribution curve of the partial coordination numbers. This shoulder can be explained by the assumption that in the liquid eutectic alloy there exist clusters with a structure similar to solid  $\text{Al}_2\text{Cu}$ . As can be seen from Fig. 7, a Cu atom has eight nearest Al neighbors in the solid state.

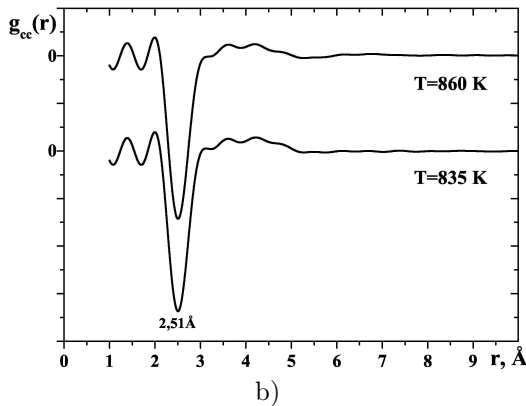
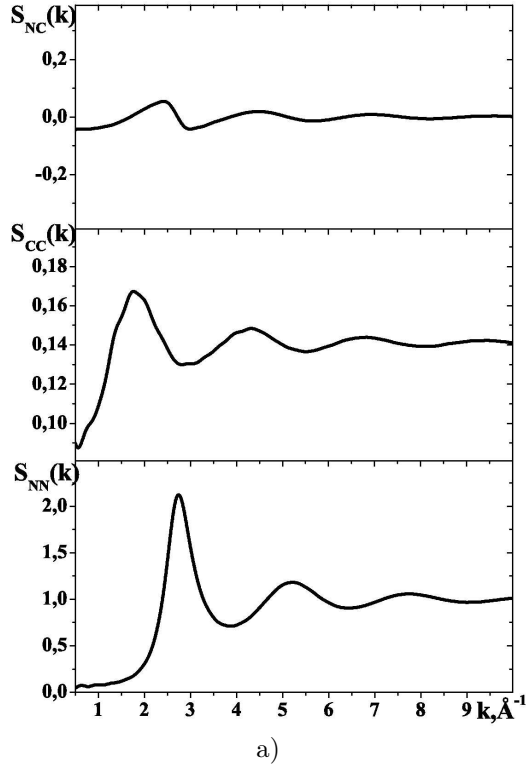


Fig. 6. The Bhatia-Thornton partial structure factors (a) and correlation functions (b) for the liquid  $\text{Al}_{0.83}\text{Cu}_{0.17}$  eutectic alloy (MD simulation).

In Fig. 6 we present the Bhatia–Thornton partial structure factors [17]. The first maxima of  $S_{CC}(k)$  and  $S_{NC}(k)$  are an order of magnitude smaller than that of  $S_{NN}(k)$ . It is known that for an ideal mixture,  $S_{CC}(k)$  is equal to the product of concentrations and  $S_{NC}(k)$  is equal to zero for all values of the wave vector.  $S_{NC}(k)$  can be seen to characteristically oscillate around zero. This is a consequence of the fact that in an eutectic melt, the

local number density of Al and Cu atoms around any Al atom differs from the corresponding density around a Cu atom. Thus, one can conclude that the deviation of the  $\text{Al}_{0.83}\text{Cu}_{0.17}$  eutectic melt from an ideal mixture is significant.

The radial concentration-concentration function,  $\rho_{CC}(r)$ , is obtained by Fourier-transforming  $S_{CC}(k)$  to  $r$ -space. For distances where self-coordination is favorable,  $\rho_{CC}(r)$  assumes positive values, whereas whenever unlike neighbors are preferred, its values are negative. As can be seen in Fig. 6, the negative peak at 2.51 Å indicates the preferred hetero-coordination of the nearest neighbors.

The changes in the number-number partial structure factors can be attributed to a variation of the spatial extent  $\xi$  of topological ordering. This parameter can be estimated from the breadth of the first peak of the number-number partial structure factor using the Scherrer particle size broadening relation  $\xi = 2\pi/\Delta s_{NN}$ . This parameter decreases smoothly with an increase in temperature. The spatial extent of chemical ordering deduced from the breadth of the first peak of the concentration-concentration partial structure factor is smaller than the spatial extent of topological ordering.

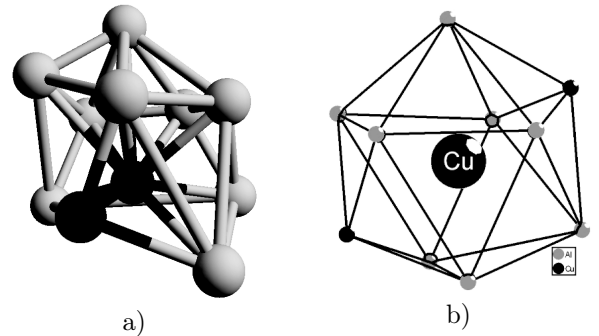


Fig. 7. A cluster of the liquid eutectic alloy (a) in comparison with a coordination polyhedron (b) for the  $\text{Al}_2\text{Cu}$  compound (MD simulation).

Figure 7 shows a comparison of a possible cluster of the liquid eutectic alloy compared with a coordination polyhedron for  $\text{Al}_2\text{Cu}$  compound demonstrating that the liquid cluster is similar to a coordination polyhedron.

#### IV. CONCLUSIONS

The diffraction study of the  $\text{Al}_{0.83}\text{Cu}_{0.17}$  eutectic alloy implies inhomogeneous atomic distribution in the liquid state at the temperatures close to the crystallization point. Molecular dynamics calculations confirm the presence of this kind of structure. The analysis of partial structure factors obtained by means of molecular dynamics showed a significant influence of the  $\text{Al}_2\text{Cu}$ -like chemical ordering on the atomic distribution in the eutectic melt. It was shown that  $\text{Al}_2\text{Cu}$  nanogroups are formed and distributed in the Al matrix.

The obtained results can be used in order to control the nucleation process during the production of new Al-based composite materials.

- [1] E. L. Rooy, *Metals Handbook. Vol. 15* (ASM International, Materials Park, Ohio, 1988).
- [2] J. E. Spinelli, D. M. Rosa, I. L. Ferreira, A. Garcia, *Mater. Sci. Eng. A* **383**, 271 (2004).
- [3] A. Guinier, *Ann. Phys.* **12**, 161 (1939).
- [4] G. D. Preston, *Philos. Mag.* **26**, 855 (1938).
- [5] D. T. Cromer, J. T. Waber, *Acta Cryst* **18**, 104 (1965).
- [6] J. Krogh-Moe, *Acta Cryst.* **9**, 951 (1956).
- [7] J. Dziedzic, M. Rychcik-Leyk, J. Rybicki, *J. Non-Cryst. Sol.* **354**, 4309 (2008).
- [8] M. Bialoskorski, J. Rybicki, in *Proc. of 8-th Workshop of PTSC* (Gdansk-Sobieszewo, 2001), p. 8.
- [9] J. Dziedzic, J. Rybicki, *J. Non-Cryst. Sol.* **354** 4316 (2008).
- [10] A. P. Sutton, J. Chen, *Philos. Mag. Lett.* **61**, 139 (1990).
- [11] H. Rafii-Tabar, A. Sutton, *Philos. Mag. Lett.* **63**, 217 (1991).
- [12] S. R. Elliot, *Nature* **354**, 445 (1991).
- [13] J. Brillo *et al.*, *J. Non-Cryst. Sol.* **352**, 4008 (2006).
- [14] M. Maret, T. Pomme, A. Pasturel, *Phys. Rev. B* **42** 1598 (1990).
- [15] S. Das, J. Horbach, M. Koza, S. Mavila Chatoth, A. Meyer, *Appl. Phys. Lett.* **86**, 11918-1 (2005).
- [16] T. E. Faber, J. M. Ziman, *Philos. Mag.* **11**, 153 (1965).
- [17] A. B. Bhatia, D. E. Thornton, *Phys. Rev. B* **2**, 3004 (1971).

### ВЗАЄМОЗВ'ЯЗОК СТРУКТРИ ЕВТЕКТИЧНОГО СПЛАВУ Al-Al<sub>2</sub>Cu В РІДКОМУ ТА КРИСТАЛІЧНОМУ СТАНАХ

С. Мудрий<sup>1</sup>, І. Штаблавий<sup>1</sup>, Я. Рибіцкі<sup>2,3</sup>

<sup>1</sup>*Кафедра фізики металів, Львівський національний університет імені Івана Франка,  
вул. Кирила і Мефодія, 8, Львів, 79005, Україна*

<sup>2</sup>*Факультет технічної фізики та прикладної математики, Гданський технічний університет,  
вул. Нарutowіча, 11/12, Гданськ, 80-952, Польща*

<sup>3</sup>*Інститут мехатроніки, нанотехнологій та вакуумної техніки, Технічний університет м. Кошалін,  
вул. Снядецьких, 2, Кошалін, 75-453, Польща*

Досліджено структуру евтектичного сплаву Al<sub>0.83</sub>Cu<sub>0.17</sub> в рідкому стані методами дифракції рентгенівських променів і молекулярної динаміки. Проаналізовано загальні та парціальні структурні фактори. Ці функції використані для обчислення парних кореляційних функцій. За результатами аналізу цих функцій встановлено існування в розплаві Al<sub>0.83</sub>Cu<sub>0.17</sub> мікрогрупувань зі структурою, близькою до Al<sub>2</sub>Cu, які розподілені в матриці на основі алюмінію.